Correlation of an Adenine-Specific Conformational Change with the ATP-Dependent Peptidase Activity of *Escherichia coli* Lon†

Jessica Patterson,‡,§ Diana Vineyard,‡,§ Jennifer Thomas-Wohlever,‡ Ramona Behshad,‡ Morris Burke,|| and Irene Lee*,‡

Department of Chemistry and Department of Biology, Case Western Reserve University, Cleveland, Ohio 44106

Received December 2, 2003; Revised Manuscript Received March 12, 2004

ABSTRACT: *Escherichia coli* Lon, also known as protease La, is a serine protease that is activated by ATP and other purine or pyrimidine triphosphates. In this study, we examined the catalytic efficiency of peptide cleavage as well as intrinsic and peptide-stimulated nucleotide hydrolysis in the presence of hydrolyzable nucleoside triphosphates ATP, CTP, UTP, and GTP. We observed that the k_{cat} of peptide cleavage decreases with the reduction in the nucleotide binding affinity of Lon in the following order: ATP > CTP > GTP ∼ UTP. Compared to those of the other hydrolyzable nucleotide triphosphates, the ATPase activity of Lon is also the most sensitive to peptide stimulation. Collectively, our kinetic as well as tryptic digestion data suggest that both nucleotide binding and hydrolysis contribute to the peptidase turnover of Lon. The kinetic data that were obtained were further put into the context of the structural organization of Lon protease by probing the conformational change in Lon bound to the different nucleotides. Both adenine-containing nucleotides and CTP protect a 67 kDa fragment of Lon from tryptic digestion. Since this 67 kDa fragment contains the ATP binding pocket (also known as the α/β domain), the substrate sensor and discriminatory (SSD) domain (also known as the α-helical domain), and the protease domain of Lon, we propose that the binding of ATP induces a conformational change in Lon that facilitates the coupling of nucleotide hydrolysis with peptide substrate delivery to the peptidase active site.

Lon, also known as protease La, is an oligomeric ATP-dependent protease which functions to degrade abnormal and certain short-lived regulatory proteins in the cell (*1*−*9*). Lon represents one of the simplest forms of ATP-dependent proteases because both the ATPase and the protease domain are located within each monomeric subunit (*10*, *11*). The functional form of *Escherichia coli* Lon has been shown to exist as a tetramer or an octamer, depending on the buffer composition (*3*). Recently, the crystal structure of an inactive mutant of the Lon protease domain has been reported. This hexameric structure lacks the ATPase domain and contains an active site Ser to Ala mutation. The structure of this protein displays a central cavity, which is commonly found in the ATPase and protease subunits of other ATP-dependent proteases (*12*). In addition to the protease domain, the structure of the α-subdomain of the ATPase subunit of Lon has been determined. This subdomain constitutes the last 25% of the carboxyl region of the intact ATPase domain of Lon; however, it lacks the conserved Walker motifs found in ATP binding proteins (*12*, *13*). Nevertheless, a structural model consisting of the α-subdomain and the protease domain of Lon could be superimposed on the HslUV structure (*12*), thereby validating the utilization of HslU as a structural model in studying the ATP-dependent peptidase reaction of Lon.

The heterosubunit ATP-dependent protease HslU/HslV is a bacterial homologue of the proteasome (*14*). It contains an oligomeric ATPase subunit and an oligomeric protease subunit which assemble to form a functional enzyme (*15*−*17*). The HslU subunit is an ATPase that functions to unfold and translocate polypeptide substrates through the central cavities of the oligomeric enzyme by a threading mechanism (*18*−*20*). In light of the structural similarities shared by Lon and HslU/HslV, as well as the high degree of sequence homology in the ATPase domains of the two enzymes (*21*), it is conceivable that Lon also couples ATP hydrolysis with substrate unfolding and translocation. Furthermore, due to their sequence homology with many AAA+ (ATPase-associated cellular activities) proteins, both Lon and HslU are classified as AAA+ proteins (*21*). The AAA+ motif typically contains an ATP binding site in the α/β-domain and a substrate sensor and discriminatory (SSD) site in the α-helical domain. It is believed that the movements of these two domains initiate chemical energy transduction in enzyme catalysis (*21*, *22*).

The structural data on Lon cannot conclusively demonstrate that it possesses an ATP-dependent peptide translocation step. However, we have obtained kinetic data to support the existence of such a mechanism. In our earlier studies, we reported that the k_{cat} of the degradation of a

† This work was supported in part by NIH Grant GM067172 and the PRI award sponsored by the Ohio Board of Regents. R.B. is the recipient of the SPUR fellowship, a program sponsored by the Howard Hughes Medical Institute.

* To whom correspondence should be addressed. Phone: (216) 368-6001. Fax: (216) 368-3006. E-mail: ixl13@po.cwru.edu.

‡ Department of Chemistry.

§ These authors contributed equally to the preparation of the manuscript.

|| Department of Biology.

10.1021/bi036165c CCC: $27.50
Published on Web 05/15/2004

defined peptide (S3)[1] by Lon is maximized by ATP hydrolysis. The defined model peptide substrate (S3) and its nonfluorescent analogue (S2) were previously used as simplified mimics of the *E. coli* Lon substrate, the lambda N protein, to demonstrate that catalytic turnover of peptide cleavage exhibits a dependence on ATP hydrolysis (*23*, *24*). Since these model peptides lack any defined secondary structure (*24*), the observed ATPase dependency could reflect a peptide translocation step (*18*−*20*, *25*, *26*). Using product inhibition studies, we further demonstrated that the inhibitory effect of ADP toward Lon could be alleviated by increasing peptide substrate concentrations. This result allowed for the construction of a minimal kinetic model to account for the ATPase-coupled peptide translocation step prior to substrate cleavage (*23*). According to our model, ATP hydrolysis could be used to thread the unfolded peptide substrate through the central cavity of the oligomeric enzyme, thereby delivering the substrate to the proteolytic site. The nonhydrolyzable ATP analogue, AMPPCP, cannot support peptide cleavage because of the lack of energy transduction. Another nonhydrolyzable analogue, AMPPNP, supports peptide cleavage with an efficiency reduced compared to that of ATP. Peptide cleavage occurs because the structure of the AMPPNP−magnesium complex may have mimicked a transition state in ATP hydrolysis, thus inducing a conformational change in Lon allowing for the delivery of the peptide (*27*). However, because AMPPNP is not hydrolyzed by Lon, the substrate translocation step is less efficient due to a lack of energy transduction.

As NTP-activated casein degradation is accompanied by hydrolysis of the respective nucleotide (at 0.5 mM nucleotide), it is conceivable that the observed differences in the respective NTPase-dependent reactions are attributed to the differences in the nucleotide base structure. Therefore, under saturating NTP conditions, Lon will exist primarily as the Lon−NTP form, and the functional relationship between the k_{cat} of NTP hydrolysis and peptidase activation could be quantitatively measured. Our proposed reaction model predicts that at saturating NTP concentrations, the hydrolyzable nucleotides that bind with weaker affinity to Lon than ATP will support peptide degradation with accompanying hydrolysis of the nucleotide triphosphate backbone. Furthermore, the k_{cat} for S3 cleavage with the hydrolyzable nucleotides should be at least comparable to or higher than that with the nonhydrolyzable ATP analogue-mediated reaction if energy transduction affects peptide translocation. To test our hypothesis, we measured the steady-state kinetic parameters for S3 cleavage in the presence of ATP, GTP, CTP, or UTP, as well as the NTPase activity of Lon in the absence and presence of S3. Since the kinetic parameters of ATP- and AMPPNP-mediated S3 degradation have been previously determined (*23*), results obtained from this study could be readily compared with our previous observations. The kinetic data that were obtained were further put into the context of the structural organization of Lon protease by probing the conformational change in Lon bound to different nucleotides using limited tryptic digestion analyses. Combining the kinetic data and the limited tryptic digestion data allowed us to evaluate the functional role of a nucleotide-specific conformational change in Lon as well as to quantify the functional relationship between NTP hydrolysis and peptidase activation.

EXPERIMENTAL PROCEDURES

Materials. ATP (lot A-7699) was purchased from Sigma, while CTP (lot 2077F), GTP (lot 9311C), and UTP (lot 6688F) were purchased from ICN. The [α-^{32}P]ATP, [α-^{32}P]-CTP, [α-^{32}P]GTP, and [α-^{32}P]UTP were purchased from Perkin-Elmer. Fmoc-protected amino acids, Boc-Abz, Fmoc-protected Lys Wang resin, and HBTU were purchased from Advanced ChemTech and NovaBiochem. HATU was purchased from PerSeptive Biosystem. Tris buffer, PEI-cellulose TLC plates, ammonium molybdate, sodium citrate, malachite green oxalate salt, cell culture media, IPTG, SBTI, TPCK-treated trypsin, PMSF, and chromatography media were purchased form Fisher, Sigma, and ACROS Organic.

General Methods. Peptide synthesis and protein purification procedures were performed as described previously (*23*). All enzyme concentrations were reported as Lon monomer concentrations.

NTP-Dependent Peptidase Assays. Steady-state velocity data were collected on a Fluoromax 3 spectrofluorimeter (Horiba Group) as described previously (*23*). Assays contained 50 mM Tris-HCl (pH 8.1), 5 mM magnesium acetate, 5 mM DTT, and 125 nM *E. coli* Lon except in experiments using GTP, where 200 nM *E. coli* Lon was used, with varying concentrations (from 0 to 1 mM) of nucleotide (ATP, CTP, GTP, and UTP) or peptide substrate S3 (from 50 to 500 μM). All assays were performed at least in triplicate, and the averaged value of the rates determined for each set of nucleotide and peptide concentrations was fit to eq 1 as described previously (*23*) using the nonlinear program EnzFitter (Biosoft).

$$v = \frac{V_{max}[A]^n[B]}{(K_{ib}K'_a + K'_a[B] + K_b[A]^n + [A]^n[B])} \quad (1)$$

where v is the observed rate, V_{max} is the maximal rate, A is the peptide substrate, B is the nucleotide, K_a is the Michaelis constant for A, K_{ib} is the intrinsic dissociation constant for B, and K_b is the Michaelis constant for B. The k_{cat} value was determined by dividing V_{max} with the concentration of the Lon monomer. The K_m values for peptide hydrolysis were calculated from the relationship $\log K'_a = n \log K_m$, where n is the Hill coefficient.

Radiolabeled NTPase Assays. Steady-state velocity data for nucleotide hydrolysis were measured as described elsewhere (*28*), and all reactions were performed at least in triplicate. Briefly, for the NTPase measurements, each reaction mixture (50 μL) contained 50 mM Tris-HCl (pH 8.1), 5 mM magnesium acetate, 2 mM DTT, and 150 nM Lon monomer for ATP or UTP and 600 nM Lon monomer for CTP or GTP. For the peptide-stimulated NTPase reac-

[1] Abbreviations: AMPPNP, adenylyl 5-imidodiphosphate; AMPPCP, adenylyl (β,γ-methylene)diphosphonate; DTT, dithiothreitol; Abz, anthranilamide; Bz, benzoic acid amide; NO_2, nitro; Tris, 2-amino-2-(hydroxymethyl)-1,3-propanediol; amp, ampicillin; KP_i, potassium phosphate; λ N (lambda N protein), lambda phage protein that allows *E. coli* RNA polymerase to transcribe through termination signals in the early operons of the phage; SE, standard error; S2, nonfluorescent analogue of S3 that is cleaved by Lon in the same manner as S3 [YRGITCSGRQK(Bz)]; S3, mixed peptide substrate containing 10% of the fluorescent peptide Y(NO_2)RGITCSGRQK(Abz) and 90% S2; NTP, nucleotide triphosphate.

tions, 500 μM peptide substrate (S2) was added to each reaction mixture, and the reactions were initiated by the addition of NTP. Subsequently, 5 μL aliquots were quenched in 10 μL of 0.5 N formic acid at seven time points (from 0 to 12 min). A 3 μL aliquot (ATPase) or 2 μL aliquot (CTPase, GTPase, and UTPase) of the reaction was spotted directly onto a PEI-cellulose TLC plate (10 cm $\times$ 20 cm) and the plate developed in 0.3 M potassium phosphate buffer (pH 3.4). Radiolabeled NDP nucleotide was then quantified using the Packard Cyclone storage phosphor screen Phosphor imager purchased from Perkin-Elmer Life Science. To compensate for slight variations in spotting volume, the concentration of the NDP product obtained at each time point was corrected using an internal reference as shown in eq 2.

$$[\mathrm{NDP}] = \left(\frac{\mathrm{NDP_{dlu}}}{\mathrm{NTP_{dlu}} + \mathrm{NDP_{dlu}}}\right)[\mathrm{NTP}] \quad (2)$$

The kinetic parameters were determined by fitting the k_{obs} data with eq 3 using the nonlinear regression program KaleidaGraph (Synergy).

$$k_{obs} = \frac{k_{obs,max}[\mathrm{B}]}{K_m + [\mathrm{B}]} \quad (3)$$

where k_{obs} is the observed rate constant, $k_{obs,max}$ is the maximal rate, B is the nucleotide, and K_m is the Michaelis−Menten constant.

Malachite Green NTPase Assays. Steady-state velocity data for ATP or CTP hydrolysis were also measured using a modified assay to detect inorganic phosphate (P_i) release (*28*, *29*). Solutions containing 0.045% (w/v) malachite green oxalate (MG) in deionized water, 4.2% (w/v) ammonium molybdate (AM) in 4 N HCl, 2% (v/v) Triton X-100 in deionized water, and 34% (w/v) sodium citrate$\cdot 2H_2O$ in deionized water were prepared. Prior to each NTPase assay, a 3:1 mixture of MG and AM was made, stirred for at least 20 min, and filtered through filter paper. The Triton X-100 solution was then added to this MG/AM solution in the amount of 100 μL per 5 mL of MG/AM solution. A solution of $NaHPO_4$ and NaH_2PO_4 (pH 8.1) was used for the calibration standard. For the NTPase measurements, we used a 210 μL reaction mixture containing 50 mM Tris-HCl (pH 8.1), 5 mM magnesium acetate, 2 mM DTT, various concentrations of Lon protease (125 nM for ATP), and 500 μM peptide substrate (S2, the nonfluorescent analogue of S3) for the peptide-stimulated NTPase assays. For all assays, the NTPase reaction was initiated by the addition of the nucleotide to the reaction mixture. At eight time points (from 0 to 15 min), a 25 μL aliquot was thoroughly mixed with 400 μL of an MG/AM/Triton X-100 solution. After 30 s, 50 μL of 34% sodium citrate was added for color development. The absorbance was then recorded at 660 nm on a UV−vis spectrophotometer for each time point. The amount of P_i formed at each time point was determined by comparing the absorbance of the sample to a P_i calibration curve. Initial velocities were determined from plots of the amount of P_i released versus time. The kinetic parameters were determined by fitting the averaged rate data with eq 3.

Tryptic Digestions. Tryptic digest reactions in mixtures containing 1.5 μM Lon, 50 mM Tris (pH 8.1), 5 mM magnesium acetate, 2 mM DTT, with or without 800 μM S2 peptide, and either 1 mM ATP, ADP, or AMPPNP, 2 mM CTP or GTP, or 3 mM UTP were started by the addition of 1/50 (w/w) TPCK (*N*-*p*-tosyl-L-phenylalanine chloromethyl ketone)-treated trypsin with respect to Lon. At 15 and 30 min, a 3 μL reaction aliquot was quenched in 3 μg of soybean trypsin inhibitor (SBTI) followed by boiling. The quenched reactions were then resolved by 12.5% SDS−PAGE analysis and visualized with Coomassie brilliant blue.

Identification of Tryptic Digestion Sites in Lon by Peptide Sequencing. The trypsin cleavage sites in Lon were identified by sequencing the Lon fragments generated by limited tryptic digestion in the presence of 1 mM ATP or GTP. After 45 min, the reactions were quenched with PMSF (phenylmethanesulfonyl fluoride) followed by boiling, and then resolved on a denaturing 4 to 15% gradient gel. The Lon fragments were electroeluted onto a PVDF membrane and sequenced by Edman degradation performed by the Molecular Biotechnology Core at the Lerner Research Institute of the Cleveland Clinic (Cleveland, OH). The first five amino acids at the amino termini of each Lon fragment were determined and then matched against the primary amino acid sequence of *E. coli* Lon [GenBank accession number P08177 (*3*)] to identify the respective trypsin cleavage sites.

RESULTS

Steady-State Kinetic Analysis of Peptide Cleavage. Using the fluorescent peptidase assay previously employed to compare the kinetics of ATP- versus AMPPNP-mediated peptide degradation (*23*), we determined the kinetic constants of ATP-, CTP-, UTP-, and GTP-mediated S3 hydrolysis by *E. coli* Lon. The NTP-dependent S3 hydrolysis reactions were monitored by the increase in fluorescence, which reflects the amount of peptide hydrolyzed over time. The steady-state observed rate constants of S3 cleavage ($k_{obs,S3}$) were determined at varying concentrations of S3 and saturating concentrations of the respective NTP. Under these conditions, Lon exists predominantly in the Lon−NTP form, and thus, the observed differences in the NTP-dependent peptidase activities reflect the effect of nucleotide hydrolysis rather than binding. Plotting $k_{obs,S3}$ as a function of S3 concentrations yields sigmoidal plots as shown in Figure 1A. On the other hand, plotting k_{obs} of S3 hydrolysis at saturating S3 and increasing NTP concentrations yields hyperbolic plots (Figure 1B). The $k_{obs,S3}$ values were also measured at varying concentrations of NTP at several fixed peptide concentrations, and the full set of velocity data was fitted with eq 1 to yield the kinetic constants summarized in Table 1. The detection of sigmoidal kinetics at fixed nucleotide but varying peptide concentrations indicates that the peptide concentration term shown in eq 1 is associated with a Hill coefficient (*23*). Since Lon functions as an oligomer, the detection of a Hill coefficient of >1 at increasing peptide concentrations suggests that the enzyme subunits communicate with each other during peptide cleavage, and the further binding of peptide substrate stimulates peptide hydrolysis.

As summarized in Table 1, both the $K_{m,S3}$ and n values vary only slightly among the different NTP-mediated peptidase reactions, indicating these parameters are not affected by nucleotide binding or hydrolysis. The K_{ib} and K_b values of the different nucleotides represent the intrinsic dissociation constant and Michaelis constant of the individual nucleotide

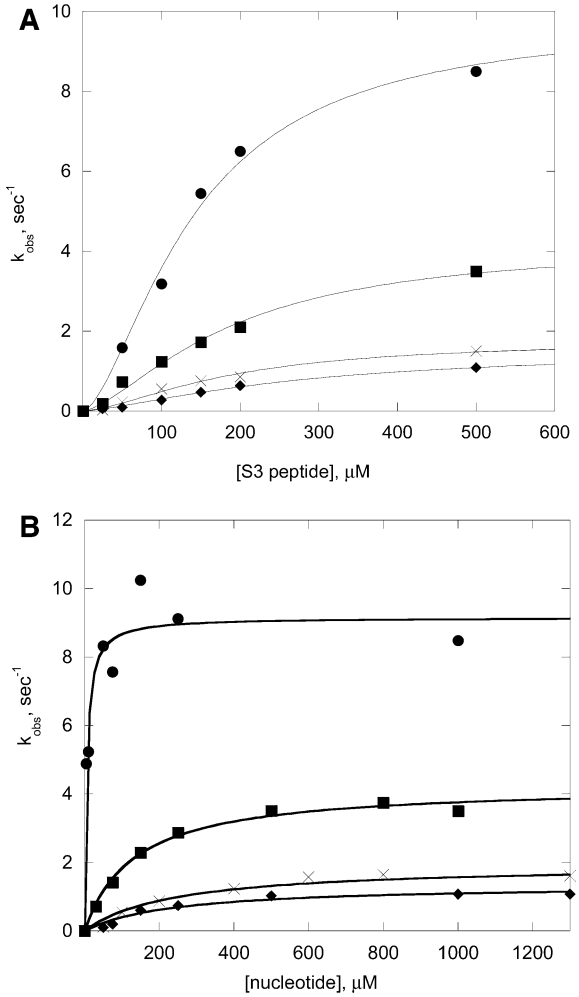

FIGURE 1: Steady-state peptidase activity of Lon in the presence of different NTPs. (A) Lon was preincubated with 25, 50, 100, 150, 200, and 500 μM S3 prior to the addition of 1 mM ATP (●), CTP (■), and GTP (◆) and 1.6 mM UTP (×). All assays were performed in triplicate, and the averaged k_{obs} values were plotted against the corresponding S3 concentration. The data were best fit with the Hill equation $k_{obs} = (k_{obs,max}[S]^n)/([S]^n K_m)$, where k_{obs} is the observed steady-state rate constant, $k_{obs,max}$ is the maximum observed steady-state rate constant, [S] is the concentration of the peptide, and n is the Hill coefficient (*30*). (B) Lon was preincubated with 500 μM S3 prior to addition of 5, 10, 50, 75, 150, and 250 μM and 1 mM ATP (●), 30, 75, 150, 200, 500, and 800 μM and 1 mM CTP (■), 50, 75, 150, 250, and 500 μM and 1 mM GTP (◆), and 100, 200, 400, 600, and 800 μM and 1.6 mM UTP (×). All assays were performed in triplicate, and the average k_{obs} values were plotted against the corresponding NTP concentration. The data were best fit with eq 3.

Table 1: Steady-State Kinetic Parameters of NTP-Dependent Cleavage of S3 by Lon

nucleotide	$k_{cat,S3} \pm$ SE (s^{-1})	$K_{m,S3} \pm$ SE (M)	$K_b \pm$ SE (M)	$K_{ib} \pm$ SE (M)	n
ATP	9.0 ± 0.5	102 ± 30	7 ± 1	7.4 ± 2	1.6
CTP	4.2 ± 0.1	151 ± 43	100 ± 20	73 ± 14	1.52
UTP	1.9 ± 0.2	99 ± 32	350 ± 125	389 ± 112	1.43
GTP	1.7 ± 0.2	219 ± 43	200 ± 78	250 ± 92	1.6
AMPPNP[a]	1.0 ± 0.1	77 ± 7	ND[b]	10 ± 1	1.6

[a] These values were obtained from ref *23*. [b] Not determined.

(*30*), respectively. These values vary for the different NTPs. According to Table 1, the K_{ib} of each NTP approximates its K_b value, indicating that the Michaelis constant reflects the intrinsic binding affinity of the nucleotide for Lon. The $k_{cat,S3}$ for the different NTPs also varies with the chemical structure of the nucleotide that is used (Table 1). Comparing the $k_{cat,S3}$ values of the peptidase reactions in Table 1 reveals the order of the ability of different nucleotides to activate S3 cleavage: ATP > CTP > UTP ~ GTP > AMPPNP. With the exception of AMPPNP, the decreasing order in $k_{cat,S3}$ mediated by different NTPs correlates with the decreasing affinities of Lon for the respective nucleotides that are represented by K_{ib} and K_b (Table 1): ATP ~ AMPPNP > CTP > GTP > UTP. Although both ATP and AMPPNP bind to Lon with comparable affinity, they exhibit different stimulatory effects toward S3 degradation. On the other hand, CTP, which has a weaker affinity for Lon than AMPPNP, exhibits a 4.2-fold higher value of $k_{cat,S3}$. Comparing the structures of the nucleotide bases reveals that both ATP and CTP share similarities in the N6 (in ATP) and N4 (in CTP) amino groups in the pyrimidine ring. Therefore, it is likely that the binding interaction between Lon and the amino group in the nucleotides is responsible for activation of peptide hydrolysis. Although both GTP and UTP are less effective than ATP or CTP in activating S3 cleavage, the k_{cat} values of these two NTP-mediated S3 cleavages are at least comparable if not slightly higher than that of AMPPNP-mediated S3 cleavage (*23*, *24*). Collectively, these data suggest that despite the reduction in binding affinity between Lon and CTP, GTP, or UTP, the hydrolysis of the triphosphate in these nucleotides confers a catalytic advantage over the tight binding AMPPNP. This result indicates that the $k_{cat,S3}$ is not solely dependent on the affinity of Lon for the nucleotide. The similarity in the $K_{m,S3}$ values is consistent with our previous report that the peptide substrate binds to Lon independent of the nucleotide (*23*). This result is also corroborated by the observation that the limited tryptic digestion patterns of Lon are identical regardless of the presence or absence of the S3 peptide substrate and further indicate that binding of the S3 peptide does not induce any detectable conformational change in Lon.

Although Lon contains an identical peptide sequence for the ATPase site in each monomer, this oligomeric enzyme has at least two different affinities for ATP. The K_d values for the high- and low-affinity sites are 1 and 10 μM, respectively (*31*, *32*). Since the K_{ib} and K_b for ATP obtained in this study approximate 7 μM (Table 1), we have concluded that the low-affinity ATP-binding site of Lon is reported in Table 1. On the basis of this observation, we further utilized the K_{ib} values summarized in Table 1 to assess the relative affinity of Lon for the different nucleotides. It should be noted that K_{ib} values only measure the effect of nucleotide binding on activation of the peptidase activity; therefore, K_{ib} alone cannot reveal whether Lon binds to CTP, GTP, or UTP using the high- or low-affinity nucleotide-binding site.

Steady-State Characterization of the NTPase Activities of Lon. In addition to being a protease, Lon also possesses intrinsic ATPase activity that is increased in the presence of the peptide (*24*) or protein substrate (*3*, *33*). Although Lon can hydrolyze any of the NTPs used in this study in the presence and absence of casein (*34*), the kinetic parameters associated with these NTPases have not been reported. To quantitatively characterize the intrinsic and peptide-stimulated NTPase activitiy of Lon, we determined the steady-state kinetic parameters of the respective nucleotide hydrolysis in the absence and presence of the S2 peptide, the nonfluo-

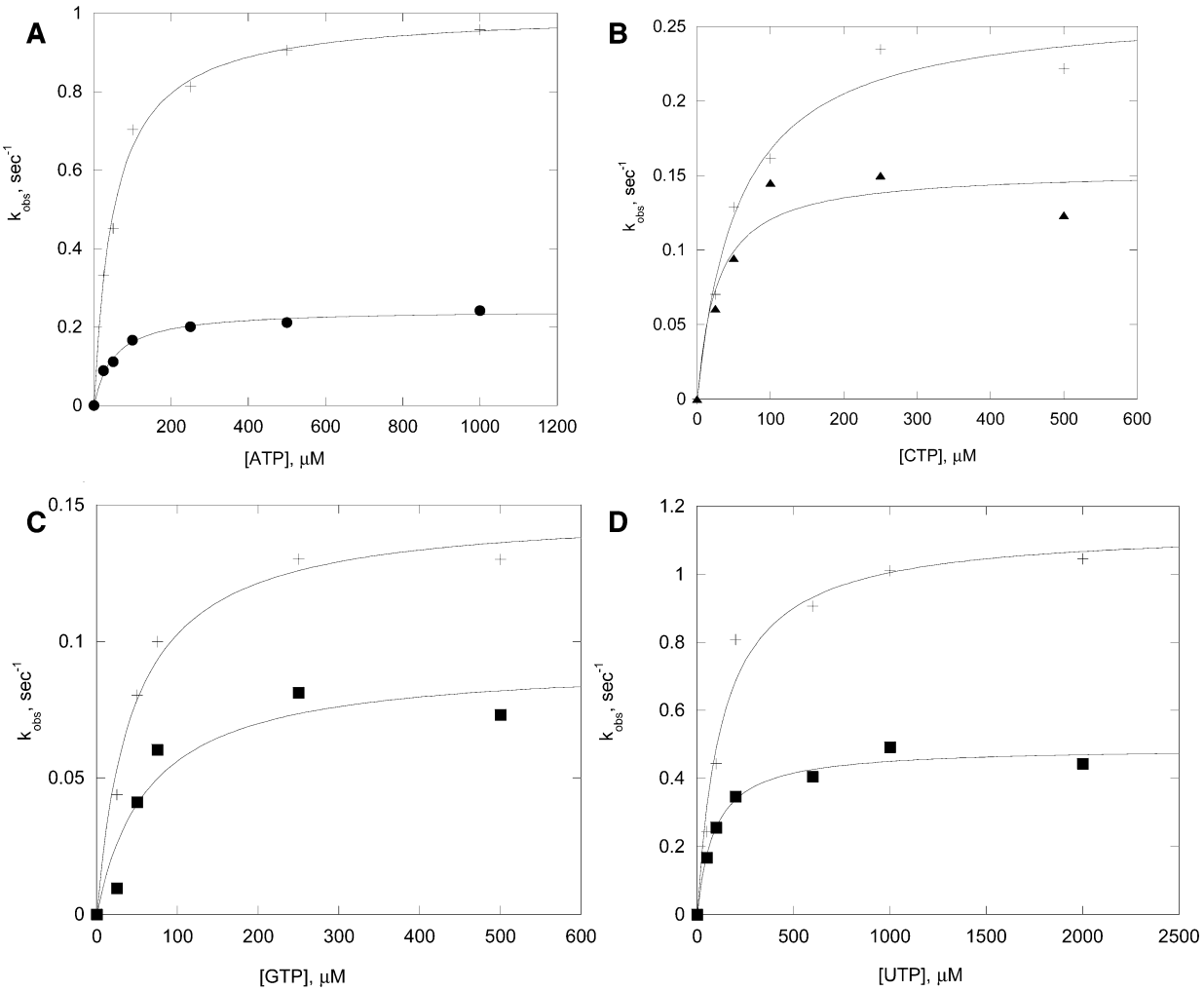

FIGURE 2: Steady-state NTPase activity of Lon in the absence and presence of 800 μM S3 peptide. The k_{obs} values for NTP hydrolysis were determined in the absence (●, ■, ▲) and presence (+) of S3 as described in Experimental Procedures. The concentrations of ATP that were used were 25, 50, 100, 250, and 500 μM and 1 mM (A). The concentrations of CTP or GTP that were used were 25, 50, 100, 250, and 500 μM. The concentrations of UTP that were used were 50, 100, 200, and 600 μM and 1 and 2 mM.

Table 2: Steady-State Kinetic Parameters of NTP Hydrolysis by Lon

	intrinsic			S2-stimulated			
nucleotide	$k_{cat,NTP} \pm$ SE (s^{-1})	$K_{m,NTP} \pm$ SE (μM)	k_{cat}/K_m(NTP) ($\times 10^3$ M^{-1} s^{-1})	$k_{cat,NTP} \pm$ SE (s^{-1})	$K_{m,NTP} \pm$ SE (μM)	k_{cat}/K_m(NTP) ($\times 10^3$ M^{-1} s^{-1})	NTPase enhancement
ATP	0.26 ± 0.02	47 ± 10	5.5	1.0 ± 0.1	49 ± 5	20	3.8
CTP	0.14 ± 0.02	60 ± 10	2.3	0.28 ± 0.02	69 ± 20	4.1	2
UTP	0.50 ± 0.02	100 ± 4	5.0	1.1 ± 0.1	132 ± 30	8.3	2.2
GTP	0.09 ± 0.02	57 ± 5	1.8	0.15 ± 0.02	42 ± 11	3.6	1.7

rescent analogue of S3 (*23*). Two different discontinuous assays were used to measure the steady-state rate constants of NTP hydrolysis ($k_{obs,NTP}$): a malachite green colorimetric assay (*28*, *29*) that monitors the release of inorganic phosphate (P_i) and an α-^{32}P-labeled ATPase assay that measures [α-^{32}P]ADP production (*28*). Plots of $k_{obs,NTP}$ as a function of nucleotide concentrations in all the NTPase experiments yielded hyperbolic plots (Figure 2). Using ATP as a reference, we have observed that the kinetic parameters obtained by the malachite green assay are comparable to those obtained by the α-^{32}P-labeled ATPase assay. Therefore, with the exception of CTPase, we used the radiolabeled NTPase assay to determine the kinetic parameters for NTP hydrolysis because less reagent was required. With regard to CTP hydrolysis, the intrinsic CTPase but not the peptide-stimulated kinetic data generated by the radiolabeled nucleotide hydrolysis assay were highly scattered. Therefore, the malachite green assay was used to determine the CTPase kinetic parameters. The plots of $k_{obs,NTP}$ versus nucleotide concentration in both the absence and presence of S2 are shown in Figure 2. All kinetic assays were performed at least in triplicate, and the averaged values at each time point were reported in each plot. In all cases, the observed rate constant data were fitted with eq 3 to yield the kinetic constants summarized in Table 2.

As discerned in Figure 2, the hydrolysis of NTPs displays Michaelis−Menten kinetics, which agrees with the detection of hyperbolic plots in the dependency of $k_{obs,S3}$ values as a function of NTP concentrations (Figure 1B). Table 2 shows that while the K_m values for both the intrinsic and S2-

stimulated NTPase reactions are comparable, the k_{cat} values vary considerably. The NTPase enhancement value is the ratio of the S2-stimulated k_{cat} to the intrinsic k_{cat} of the respective NTP, and yields an assessment of the effect of peptide substrate on NTPase stimulation (Table 2). As summarized in Table 2, the k_{cat} of the intrinsic NTPase activity is in the following order: UTP > ATP > CTP > GTP. On the other hand, the k_{cat} of the S2-stimulated NTPase activity is in the following order: ATP ~ UTP > CTP > GTP. Comparing the order of intrinsic versus peptide-stimulated k_{cat} values for the respective NTPase activities reveals that the S2 peptide exhibits a modest stimulatory effect on the ATPase activity (3.8; Table 2) compared to the CTP, GTP, and UTPase activities (1.7−2.2; Table 2). Furthermore, the k_{cat}/K_m value for ATP in the presence of the peptide substrate is higher than those of the other NTPs, thus indicating that ATP is the preferred activator.

Probing the Structural Changes in the AAA+ Motif of Lon. To correlate the kinetic data given in Tables 1 and 2 with the function(s) of the AAA+ chaperone motif in Lon (*21*, *22*), we utilized limited tryptic digestion to probe the conformational change of Lon in the absence and presence of the S2 peptide as well as different NTPs. The domain organization of *E. coli* Lon has been examined by comparing the digestion pattern of the enzyme by overnight digestion with V8 protease (*35*). Both ATP- and ADP-bound Lon are more resistant to V8 digestion than unbound Lon, suggesting that the enzyme undergoes a conformational change when binding to these nucleotides. The functional role of the ATP- or ADP-induced conformational change of Lon is not known. To address this issue, we examined the susceptibility of Lon to limited tryptic digestion under the reaction conditions used in our kinetic studies. Using trypsin rather than V8 protease as a probe, we were able to detect an adenine-specific conformational change in Lon within 30 min of digestion. The limited tryptic digestion patterns of Lon incubated in the absence and presence of 800 μM S2 peptide ($8K_{m,S3}$) and with a saturating amount of nucleotides are shown in Figure 3A. Since the NTPs are also hydrolyzed under these reaction conditions, both the Lon−NDP and Lon−NTP forms are anticipated to exist during the tryptic digestion conditions. Identical Lon fragmentation patterns were detected in the absence or presence of the nucleotide when S2 was omitted (data not shown), indicating that the peptide did not induce any conformational change in Lon that could be detected by tryptic digestion. Figure 3A shows that Lon is more resistant to tryptic digestion when incubated with ATP than with the other NTPs, suggesting that the Lon−ADP or Lon−ATP form adopts a more compact conformation. Since all the limited tryptic digestion results shown in Figure 3A most likely reflect the resistance of the Lon−NDP complex to tryptic digestion, we performed a control to further compare the stability of Lon bound to ADP or AMPPNP and without nucleotide (Figure 3B). Since AMPPNP is not hydrolyzed by Lon and it supports S3 cleavage (with reduced efficiency compared to ATP), it is used to mimic the effect of ATP bound to Lon while resisting tryptic digestion. According to Figure 3B, the fragmentation patterns of Lon incubated with ATP, ADP, and AMPPNP are comparable. However, in the digestion reaction of Lon incubated with AMPPNP, a slightly higher level of the 35 kDa fragment is detected, suggesting that AMPPNP-bound Lon might have a less compact conformation than ADP-bound Lon.

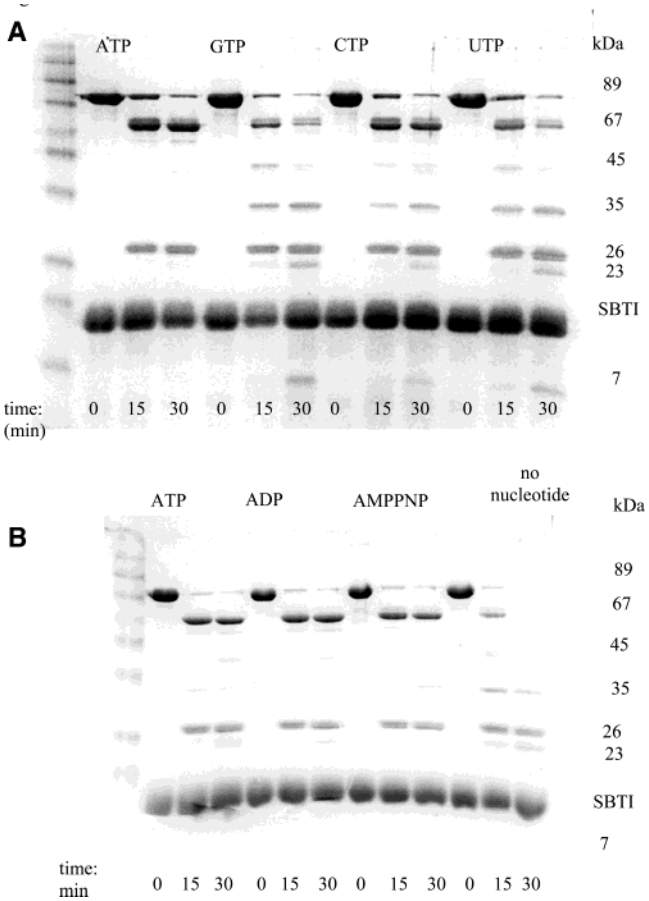

FIGURE 3: Limited tryptic digestion of Lon in the presence of nucleotides. Lon was digested with a limiting amount of trypsin and quenched at the indicated times with soybean trypsin inhibitor (SBTI) as described in Experimental Procedures. The first lane shows the molecular markers in kilodaltons (from top to bottom): 172, 110, 79, 62, 48, 37, 24, 19, 13, and 5.

Table 3: Identification of the Trypsin Digestion Sites in Lon

observed molecular mass (kDa)	sequence identified[a]	cleavage site	domains included	condition
67	AIQKE and ELGEM	A237/E241−K783	ATPase, SSD, peptidase	*b*
45	ELGEM	A237−R587	ATPase, SSD	*c*
35	LSGYT	L490−K783	SSD, peptidase	*c*
26	MNPER and SERIE	M1/S6−K236/K240	amino terminus	*b*
23	ADNEN	A588−K783	peptidase	*c*
7	LSGYT	L490−R587	SSD	*c*

[a] The first five-amino acid sequence of each Lon fragment was identified by Edman degradation as described in Experimental Procedures. [b] Detected in the absence or presence of NTPs. [c] Detected in the absence of adenine-containing nucleotides.

When tryptic digestion was performed on Lon incubated with ATP, ADP, AMPPNP, or CTP, two prominent fragments with apparent molecular masses of 67 and 26 kDa (Table 3) were detected within 15 min. In contrast, nucleotide-free Lon, as well as the GTP- and UTP-incubated Lon, was mostly digested by trypsin to yield fragments with apparent molecular masses of 67, 45, 35, 26, and 7 kDa, respectively (Table 3). Increasing the incubation time of the limited tryptic digestion reactions did not significantly alter

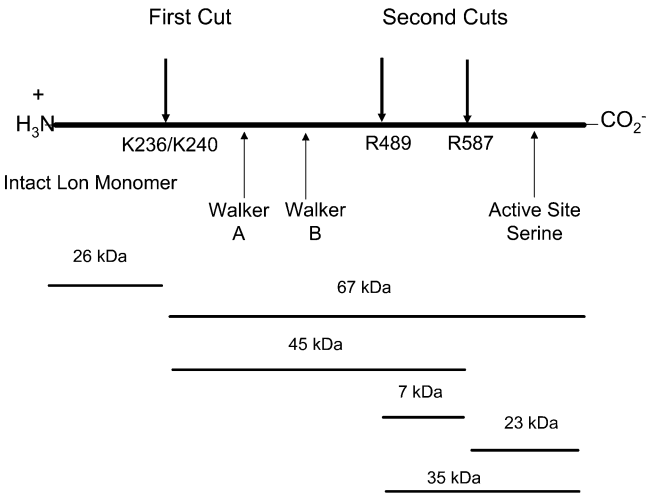

FIGURE 4: Fragmentation of Lon resulting from limited tryptic digestion. The peptide fragments generated from limited tryptic digestion were acquired as described in Experimental Procedures. The sizes of the Lon fragments were estimated on the basis of their position on the SDS gel compared to the molecular mass markers. The relative positions of the fragments compared to the intact Lon monomer were deduced from the sequencing data given in Table 3.

the digestion patterns of Lon incubated with ATP or ADP. However, the 67 and 45 kDa fragments of the reaction mixtures containing GTP, CTP, or UTP were further digested by trypsin to yield more of the 35, 23, and 7 kDa fragments (Figure 3A).

The trypsin cleavage sites identified by peptide sequencing experiments are summarized in Table 3, and the accessible trypsin cleavage sites of Lon are illustrated in Figure 4. The sizes of the tryptic digestion fragments determined by their relative mobility on the 4 to 15% gradient gel with respect to the molecular markers agreed well with the calculated molecular mass of the Lon fragments based upon the identities of the trypsin cleavage sites (Table 3). In the presence of ATP or ADP, trypsin cleaves Lon primarily at K236 or K240 to yield a 26 kDa fragment corresponding to the amino terminus of Lon and a 67 kDa fragment corresponding to the AAA+ chaperone motif and the protease domain of Lon [Figure 4 and Table 3 (*3*, *21*, *22*, *35*−*37*)]. The AAA+ chaperone motif is further comprised of the Walker A and B motifs of the ATPase domain and SSD domain found in many ATPases (*21*, *22*). When intact Lon was treated with trypsin in the presence or absence of non-adenine nucleotide triphosphates, the 67 kDa fragment was further degraded into smaller fragments (Figure 4 and Table 3). The 45 and 23 kDa fragments correspond to tryptic cleavage at R587 which separates the AAA+ chaperone domain from the peptidase domain in Lon. Tryptic cleavage of the 67 kDa fragment at R489 gave a 35 kDa fragment which contained the SSD domain and peptidase domain. The 35 kDa fragment was further cleaved by trypsin to separate the SSD domain (7 kDa) and protease domain (23 kDa). No fragment corresponding to the ATPase domain alone was detected. This could be attributed to rapid degradation of the ATPase domain by trypsin due to its relatively open conformation as observed in the non-nucleotide-bound HslU (*27*, *38*−*40*).

Modeling the Nucleotide Base Binding Site in Lon Using HslU as a Study Model. Because of the architectural similarity shared by Lon and the ATPase HslU (*12*), we have constructed a model for the nucleotide-binding site of Lon based upon the crystal structure of HslU bound to dADP (PDB entry 1HT2). We utilized the Swiss PDB viewer program to construct the nucleotide binding site for one of the monomers in HslU (the E chain) bound to dADP. This region contains Ile17−Ile66 of the E chain, which encompasses the conserved Walker A motif found in the AAA+ protein family (Figure 5A,B). Sequence alignment of *E. coli* Lon with the nucleotide binding site of HslU reveals that the residues in the Walker A motif of Lon and HslU are highly homologous (Figure 5C). This level of sequence homology validates the fitting of the Lon primary amino acid sequences flanking Ala316−Leu365 to the structure of HslU (consisting of Ile17−Ile66) to yield a model for the nucleotide binding site in Lon (Figure 5C,D). Figure 5B depicts the crystal structure of the region in HslU that interacts with the N6 amino group in adenine, whereas Figure 5D illustrates a model (based upon the sequence alignment shown in Figure 5C) showing that Lon appears to interact with the N6 amino group in ADP via the same mechanism as HslU. In HslU, the N6 amino group functions as a hydrogen bond donor that could simultaneously interact with the carbonyl oxygen in Ile18 and Val61 along the amide backbone of the enzyme. According to Figure 5C, Val61 is located within the Walker A motif and is conserved in Lon. Therefore, it is conceivable that the carbonyl oxygen of Val360 in Lon makes the same contact with the N6 amino group in adenine. Through sequence alignment, we have also identified that the carbonyl oxygen in the amide backbone of Gln317 in Lon (Figure 5D) could adopt the same function as Ile18 in HslU (Figure 5B). Taken together, our model indicates that Lon binds to the adenine nucleotide via two hydrogen bond interactions with the N6 amino group in adenine, and disruption of these interactions may affect the affinity of Lon for the nucleotide.

DISCUSSION

Lon is one of the simplest ATP-dependent proteases within the AAA+ protease family (*3*, *21*, *22*). On the basis of sequence and structural similarities shared by Lon and other ATP-dependent proteases, it is proposed that Lon also couples ATP binding and hydrolysis to unfold and translocate peptide substrates into its protease chamber. The unfolded polypeptide is threaded through the central protease chamber which is formed by oligomerization of the enzyme subunits. In previous studies, we reported that Lon exhibited ATPase dependency in hydrolyzing an unstructured peptide containing one Lon cleavage site (*24*). Through kinetic characterization of the ATP- and AMPPNP-dependent peptidase reactions, we assigned the observed ATPase dependency to an energy-coupled peptide translocation step similar to ones found in other ATP-dependent proteases (*23*). To further test this hypothesis, we compared the steady-state kinetic parameters of NTP-dependent S3 cleavage and NTP hydrolysis to evaluate the functional relationship between nucleotide binding and hydrolysis with peptide cleavage. Since CTP, GTP, and UTP also activate the proteolytic activity of Lon and are hydrolyzed during the reaction (*34*), they were used as probes to study the mechanism by which Lon transduces chemical energy generated from ATP hydrolysis into the movement of the peptide substrate into the protease chamber. At saturating nucleotide concentrations, the predominant

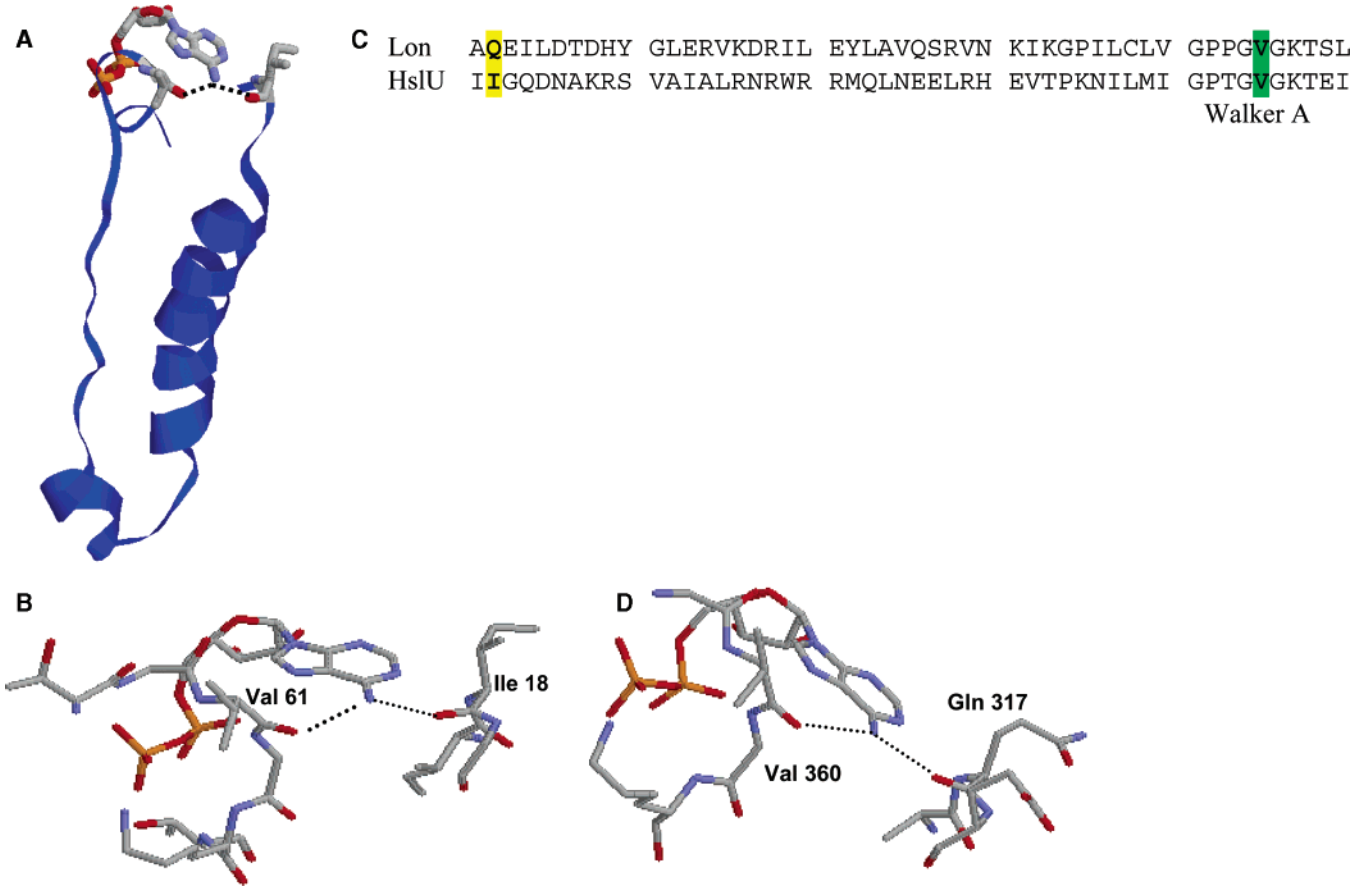

FIGURE 5: Modeling the adenine binding site of Lon based upon the structure of HslU bound to ADP (PDB entry 1HT2). (A) The structure of a monomeric HslU containing residues 16−66 is shown in blue. The structure of ADP is shown bound to the top of the cleft. (B) The N6 amino group in adenine functions as a hydrogen bond donor that can interact with the carbonyl oxygen of Ile18 and Val61 in HslU. (C) The sequences corresponding to the Walker A motif of Lon and HslU are highly conserved. This region was used as a reference point to align Ala316−Leu365 of Lon with Ile17−Ile66 of HslU. The residues that are anticipated to interact with the N6 amino group of adenine are highlighted in green and yellow. (D) On the basis of the sequence alignment, the carbonyl oxygens of Val360 and Gln317 in Lon are proposed to form hydrogen bonds with the N6 amino group in adenine.

enzyme form is the Lon−NTP form, and thus, the kinetic parameters associated with S3 cleavage should be related to the effect of nucleotide binding and/or hydrolysis. In the absence of detailed structural information revealing the different functional states of Lon, we utilized steady-state enzyme kinetic techniques to demonstrate that at least one enzyme form of Lon functions to transduce the chemical energy liberated from ATP hydrolysis to stimulate the catalytic turnover of peptide cleavage. This provides evidence for the existence of a peptide translocation step in Lon.

The kinetic parameters summarized in Tables 1 and 2 collectively indicate that the k_{cat} of peptide hydrolysis is partially coupled with energy transduction, as ATP, being the most effective peptidase activator, is the most sensitive to peptide-stimulated hydrolysis. As seen in Table 1, the k_{cat} of S3 cleavage is 9 and 4.2 s^{-1} for ATP and CTP, respectively, whereas for GTP and UTP, the k_{cat} of S3 cleavage is within the range of 1.7−1.9 s^{-1}. Despite the variation in $k_{cat,S3}$ found among the different NTPs, the $k_{cat,S3}$ values obtained for these nucleotides are higher than that obtained for AMPPNP (Table 1) (*23*). Since AMPPNP is a nonhydrolyzable analogue of ATP, it is used to evaluate the functional role of ATP binding in Lon catalysis. Comparing the relative affinity of ATP with that of AMPPNP in Table 1 reveals that Lon binds to both adenine nucleotides with comparable affinities. The K_{ib} of AMPPNP for S3 cleavage is 10 μM, which is similar to the K_{ib} for ATP (7.4 μM; Table 1) but is lower than those obtained for CTP, GTP, and UTP (73, 250, and 389 μM, respectively; Table 1). The limited tryptic digestion patterns of ATP- and AMPPNP-protected Lon also show that both nucleotides induce a more compact conformation in the enzyme than CTP, GTP, and UTP (Figure 3A,B). Collectively, these data indicate that while AMPPNP is not hydrolyzed by Lon, it still binds to Lon in a manner similar to that of ATP. Since AMPPNP induces the same conformational change in Lon as ATP or ADP, as judged by the limited tryptic digestion study (Figure 3B), the lower k_{cat} for the AMPPNP-mediated S3 hydrolysis reaction is most likely due to the lack of energy transduction associated with nucleotide hydrolysis rather than the absence of an adenine-specific conformational change. This result, in conjunction with our previous observation that AMPPCP failed to support peptide cleavage (*24*), provides quantitative evidence of the fact that at least one enzyme form of Lon couples NTP hydrolysis with peptide cleavage.

Although all the NTPs generate a k_{cat} value for S3 cleavage that is higher than that of the nonhydrolyzable analogue AMPPNP, the $k_{cat,S3}$ values for the NTPs differ from one another. This difference in $k_{cat,S3}$ loosely follows the ranking of the relative affinities of Lon for the nucleotides (K_{ib} and K_b; Table 1), the magnitude of NTPase enhancement (Table 2), and the effectiveness of the nucleotide in protecting Lon

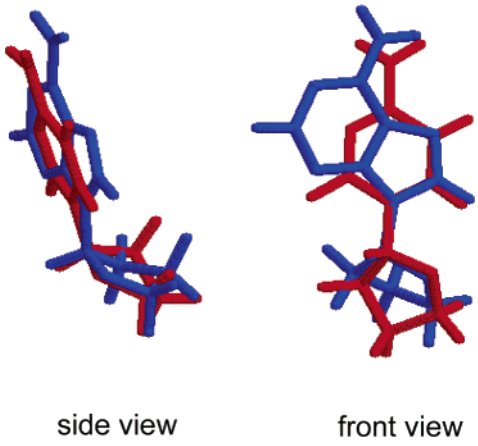

FIGURE 6: Comparison of the structures of adenine and cytidine. An overlaid view of the structures of adenine and cytidine reveals that the amino groups in the two nucleotide bases are in the spatial proximity of one another. Adenine is shown in blue and cytidine in red.

from tryptic digestion (Figure 3A). The order of peptidase activation is as follows: ATP > CTP > GTP > UTP. This order parallels the ability of the respective NTPs to protect the 67 kDa fragment of Lon from tryptic digestion: ATP > CTP > GTP ~ UTP. According to Table 1, peptide hydrolysis by Lon is more efficient in the presence of ATP and CTP, which taken together with the limited tryptic digestion data, suggests that there is an enzyme form in Lon that exhibits higher selectivity in transducing the energy liberated from ATP hydrolysis into the activation of peptidase activity.

To explain why CTP is a better peptidase activator than GTP and UTP, we constructed a structural model for the nucleotide base binding site of Lon based upon the crystal structure of HslU bound to dADP [Figure 5 (*27*, *39*, *40*)]. Figure 5D shows that the N6 amino group in adenine serves as a hydrogen bond donor that could potentially interact with the carbonyl oxygen of Gln317 and Val360 in Lon. According to this model, nucleotides capable of forming similar contacts with Lon should mimic the functions of the N6 amino group in ATP, which in this case is the induction of a closed enzyme form compared to unbound Lon. Figure 6 overlays the structure of adenosine and cytosine, which shows that both amino groups are in the spatial proximity of one another. Constrained energy minimization of ATP and CTP performed by Pate et al. showed that the two amino groups were 0.7 Å apart (*41*). Given the spatial similarity of the two amino groups in the respective nucleotides, it is conceivable that CTP could make contacts with Lon similar to those of adenine and induce a relatively closed conformational change in Lon compared to GTP and UTP. CTP, however, is not a perfect mimic of ATP, as its $k_{cat,S3}$ is 2-fold lower than that obtained for ATP and it is less effective than any of the adenine nucleotides at protecting Lon from tryptic digestion. The increase in K_b and K_{ib} for CTP (Table 1) is probably caused by the loss of interaction between Lon and other parts of the heterocyclic base in the nucleotide. These results suggest that the $k_{cat,S3}$ value is related to the compactness of the nucleotide-induced conformation in the enzyme. CTP, GTP, and UTP have lower $k_{cat,S3}$ values than ATP because they induce a less compact conformation in Lon, which reduces the effectiveness of the energy transduction process. Collectively, these data indicate a functional relationship between peptidase activation, enhanced peptide-stimulated ATPase activities, and the nucleotide-induced conformational change in the enzyme. The effective communication among these three factors is needed to optimize the peptidase activity of Lon.

Using limited tryptic digestion studies, we have demonstrated that a compact structure forms between the three functional domains of Lon, the α/β ATPase domain, the SSD domain (also known as the α-helical domain), and the peptidase domain, in the presence of ATP, ADP, or AMP-PNP, that resists tryptic digestion. These results agree well with the report on the domain organization of nucleotide-bound Lon (*35*) and HslU/HslV (*27*). In addition to binding the polypeptide substrate, the SSD domain has been proposed to participate in ATP hydrolysis (*21*, *22*, *37*). The observed 2-fold higher peptide-stimulated ATPase enhancement (3.8; Table 2) compared to the other peptide-stimulated NTPase enhancement (~2; Table 2) could therefore be attributed to the weakened interaction between the SSD and the γ-phosphate of the NTP (*22*, *37*). Although our tryptic digestion results show that adenine nucleotides induce a closed conformation in Lon, the adenine-specific conformational change alone cannot support peptide cleavage. For example, AMPPNP is bound to Lon with an affinity comparable to that of ATP and induces a compact conformation. The $k_{cat,S3}$ of AMPPNP, however, is lower than the values obtained for the hydrolyzable nucleotides that bind to Lon with lower affinities (Table 1), which suggests that nucleotide hydrolysis also plays a role in activating peptide hydrolysis. This argument is further supported by the tryptic digestion results showing that ADP induces a compact conformation in Lon that is slightly distinguishable from the AMPPNP-bound enzyme form (Figure 3B).

Using the structural changes associated with binding of HslU to an adenine nucleotide as a template, we incorporated the data obtained in this and previous studies to discuss the role of ATP binding and hydrolysis in mediating energy transduction and peptide hydrolysis in Lon. This model features an ATPase-dependent peptide translocation and protease mechanism similar to that proposed for HslUV. The binding and hydrolysis of ATP induce a series of conformational changes in the enzyme that render peptide substrate access to the central protease cavity. Figure 7 depicts a simplified model of oligomeric Lon containing only two of the subunits which face one another to form a central cavity. It should be noted that the other monomers are omitted for clarity. Furthermore, our current model assumes that each monomeric subunit is functional as an ATP-dependent protease, and the interaction among the subunits may invoke positive cooperativity in enzyme catalysis that is characterized by a Hill coefficient of >1. However, further experiments should be conducted to further evaluate this cooperativity.

In the absence of nucleotide, Lon adopts a relatively loose conformation in which the ATPase, SSD, and peptidase domains are susceptible to tryptic digestion and yield the fragments shown in Table 3 (I in Figure 7). These loose conformations among the subunits form a narrow opening to the central cavity in Lon, thereby hindering the access of the peptide substrate to the protease chamber. The binding of ATP to the AAA+ motif in Lon induces a more compact

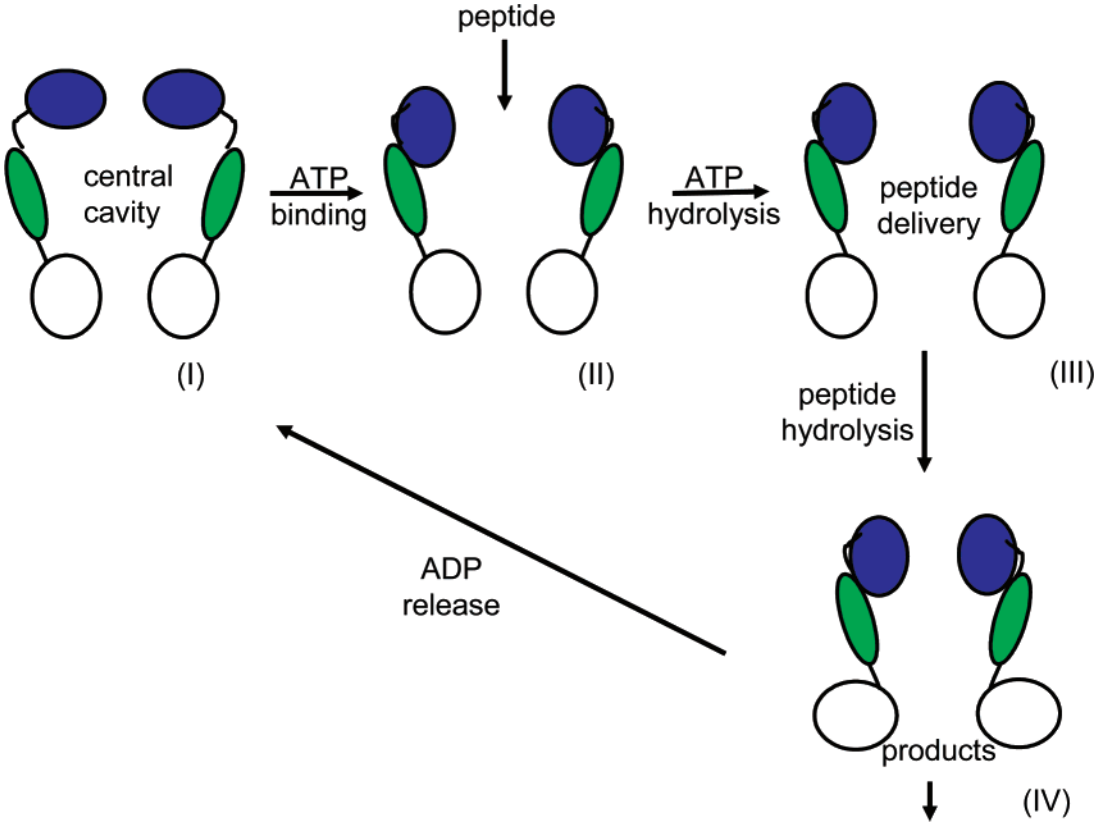

FIGURE 7: Model proposed for the different enzyme forms in Lon that couple ATP binding and hydrolysis in activating peptide hydrolysis. This model is proposed on the basis of the structural similarities shared by Lon and HslU. An ATPase-dependent peptide translocation is proposed in this model (see the Discussion). The α/*β*-subdomain and the α-helical subdomain of the AAA+ motif are in blue and green, respectively. The protease domain is in white. The protein domains and subdomains are connected by flexible linkers.

conformation within the enzyme, which is more resistant to tryptic digestion than form I (II in Figure 7). This structural rearrangement opens the pore leading into the central cavity, which renders the peptide access to the protease chamber and facilitates the transduction of chemical energy generated from ATP hydrolysis to the active site of the protease where peptide cleavage occurs (form III in Figure 7). Although this step is speculative in Lon, the coupling of ATP binding and hydrolysis to energy transduction through conformational changes in enzymes has been reported in molecular motors such as myosin (*42*) and HslUV (*27*). In our studies, the existence of this step is supported by the observed correlation between peptide-stimulated NTPase activity and the higher $k_{cat,S3}$ obtained for the hydrolyzable nucleotides compared to those of nonhydrolyzable ATP analogues. The mechanism by which Lon returns to the free enzyme form is not clear. However, on the basis of the detection of a noncompetitive inhibition pattern for one of the hydrolyzed peptide products against the S3 substrate, we propose that Lon isomerizes to another form during peptide cleavage (*23*). Since the hydrolyzed peptide product is a truncated version of the S3 substrate, it is anticipated to act as a competitive inhibitor against S3. The noncompetitive inhibition pattern seems to suggest that Lon adopts a different form upon peptide cleavage and the postcatalytic enzyme form is specific only for the hydrolyzed peptide product but not for S3. This enzyme isomerization step could account for the lack of additional S3 degradation in form IV (Figure 7).

The model proposed in Figure 7 predicts that ATP hydrolysis should occur before peptide cleavage, and adenine nucleotides lacking hydrogen donating properties at the C6 position should be poor activators of Lon. The former prediction could be readily tested by comparing the pre-steady-state kinetics of peptide and ATP hydrolysis. One anticipates that the rate constant for ATP hydrolysis will be higher than that obtained for peptide cleavage. This endeavor is currently being examined in our laboratory using the same defined peptide substrate. Elucidating the timing of ATP binding and hydrolysis should expand our mechanistic understanding of Lon. With regard to evaluating the functional role of the hydrogen bond interaction between Lon and the nucleotide base in adenine, we propose a detailed investigation utilizing non-natural nucleotides. These nucleotides lacking any hydrogen bond donating properties in the heterocyclic bases will be used as probes to evaluate the functional role of nucleotide binding in Lon. The design and synthesis of a series of non-natural nucleotides is currently underway to further address this issue.

ACKNOWLEDGMENT

We thank Dr. Anthony Berdis, Hilary Frase, and Jonathon Ipsaro for their assistance in the preparation of the manuscript.

REFERENCES

1. Chung, C. H., and Goldberg, A. L. (1981) The product of the lon (capR) gene in *Escherichia coli* is the ATP-dependent protease, protease La, *Proc. Natl. Acad. Sci. U.S.A. 78*, 4931−4935.
2. Gottesman, S., Gottesman, M. E., Shaw, J. E., and Pearson, M. L. (1981) Protein degradation in *E. coli*: the lon mutation and bacteriophage lambda N and cll protein stability, *Cell. 24*, 225−233.

3. Goldberg, A. L., Moerschell, R. P., Chung, C. H., and Maurizi, M. R. (1994) ATP-dependent protease La (lon) from *Escherichia coli*, *Methods Enzymol. 244*, 350−375.
4. Gottesman, S., Maurizi, M. R. (1992) Regulation by Proteolysis: Enegry-Dependent Proteases and Their Targets, *Microbiol. Rev. 56*, 592−621.
5. Gottesman, S. (1996) Proteases and their targets in *Escherichia coli*, *Annu. Rev. Genet. 30*, 465−506.
6. Maurizi, M. R. (1992) Proteases and protein degradation in *Escherichia coli*, *Experientia 48*, 178−201.
7. Charrette, M., Henderson, G. W., and Markovitz, A. (1981) ATP hydrolysis-dependent activity of the lon (capR) protein of *E. coli* K12, *Proc. Natl. Acad. Sci. U.S.A. 78*, 4728−4732.
8. Schoemaker, J. M., Gayda, R. C., Markovitz, A. (1984) Regulation of cell division in *Escherichia coli*: SOS induction and cellular location of the sulA protein, a key to *lon*-associated filamentation and death, *J. Bacteriol. 158*, 551−561.
9. Goff, S. A., and Goldberg, A. L. (1985) Production of abnormal proteins in *E. coli* stimulates transcription of lon and other heat shock genes, *Cell 41*, 587−595.
10. Chin, D. T., Goff, S. A., Webster, T., Smith, T., and Goldberg, A. L. (1988) Sequence of the lon gene in *Escherichia coli*. A heat-shock gene which encodes the ATP-dependent protease La, *J. Biol. Chem. 263*, 11718−11728.
11. Amerik, A., Chistiakov, L. G., Ostroumova, N. I., Gurevich, A. I., and Antonov, V. K. (1988) [Cloning, expression and structure of the functionally active shortened lon gene in *Escherichia coli*], *Bioorg. Khim. 14*, 408−411.
12. Botos, I., Melnikov, E. E., Cherry, S., Tropea, J. E., Khalatova, A. G., Rasulova, F., Dauter, Z., Maurizi, M. R., Rotanova, T. V., Wlodawer, A., and Gustchina, A. (2004) The catalytic domain of *Escherichia coli* Lon protease has a unique fold and a Ser-Lys dyad in the active site, *J. Biol. Chem. 279*, 8140−8148.
13. Botos, I., Melnikov, E. E., Cherry, S., Tropea, J. E., Khalatova, A. G., Rasulova, F., Dauter, Z., Maurizi, M. R., Rotanova, T. V., Wlodawer, A., and Gustchina, A. (2004) *J. Struct. Biol. 146*, 113−122.
14. Rohrwild, M., Coux, O., Huang, H. C., Moerschell, R. P., Yoo, S. J., Seol, J. H., Chung, C. H., and Goldberg, A. L. (1996) HslV−HslU: A novel ATP-dependent protease complex in *Escherichia coli* related to the eukaryotic proteasome, *Proc. Natl. Acad. Sci. U.S.A. 93*, 5808−5813.
15. Rohrwild, M., Pfeifer, G., Santarius, U., Muller, S. A., Huang, H. C., Engel, A., Baumeister, W., and Goldberg, A. L. (1997) The ATP-dependent HslVU protease from *Escherichia coli* is a four-ring structure resembling the proteasome, *Nat. Struct. Biol. 4*, 133−139.
16. Goldberg, A. L., Akopian, T. N., Kisselev, A. F., Lee, D. H., Rohrwild, M. (1997) New insights into the mechanisms and importance of the proteasome in intracellular protein degradation, *Biol. Chem. 378*, 131−140.
17. Yoo, S. J., Seol, J. H., Shin, D. H., Rohrwild, M., Kang, M. S., Tanaka, K., Goldberg, A. L., and Chung, C. H. (1996) Purification and characterization of the heat shock proteins HslV and HslU that form a new ATP-dependent protease in *Escherichia coli*, *J. Biol. Chem. 271*, 14035−14040.
18. Lee, C., Schwartz, M. P., Prakash, S., Iwakura, M., and Matouschek, A. (2001) ATP-dependent proteases degrade their substrates by processively unraveling them from the degradation signal, *Mol. Cell 7*, 627−637.
19. Reid, B. G., Fenton, W. A., Horwich, A. L., and Weber-Ban, E. U. (2001) ClpA mediates directional translocation of substrate proteins into the ClpP protease, *Proc. Natl. Acad. Sci. U.S.A. 98*, 3768−3772.
20. Ishikawa, T., Beuron, F., Kessel, M., Wickner, S., Maurizi, M. R., and Steven, A. C. (2001) Translocation pathway of protein substrates in ClpAP protease, *Proc. Natl. Acad. Sci. U.S.A. 98*, 4328−4333.
21. Neuwald, A. F., Aravind, L., Spouge, J. L., and Koonin, E. V. (1999) AAA+: A class of chaperone-like ATPases associated with the assembly, operation, and disassembly of protein complexes, *Genome Res. 9*, 27−43.
22. Ogura, T., and Wilkinson, A. J. (2001) AAA+ superfamily ATPases: common structure−diverse function, *Genes Cells 6*, 575−597.
23. Thomas-Wohlever, J., and Lee, I. (2002) Kinetic characterization of the peptidase activity of *Escherichia coli* Lon reveals the mechanistic similarities in ATP-dependent hydrolysis of peptide and protein substrates, *Biochemistry 41*, 9418−9425.
24. Lee, I., and Berdis, A. J. (2001) Adenosine triphosphate-dependent degradation of a fluorescent lambda N substrate mimic by Lon protease, *Anal. Biochem. 291*, 74−83.
25. Hoskins, J. R., Pak, M., Maurizi, M. R., and Wickner, S. (1998) The role of the ClpA chaperone in proteolysis by ClpAP, *Proc. Natl. Acad. Sci. U.S.A. 95*, 12135−12140.
26. Reid, B. G., Fenton, W. A., Horwich, A. L., Weber-Ban, E. U. (2001) ClpA mediates directional translocation of substrate proteins into the ClpP protease, *Proc. Natl. Acad. Sci. U.S.A. 98*, 3768−3772.
27. Wang, J., Song, J. J., Seong, I. S., Franklin, M. C., Kamtekar, S., Eom, S. H., and Chung, C. H. (2001) Nucleotide-dependent conformational changes in a protease-associated ATPase HsIU, *Structure 9*, 1107−1116.
28. Gilbert, S. P., and Mackey, A. T. (2000) Kinetics: a tool to study molecular motors, *Methods 22*, 337−354.
29. Lanzetta, P. A., Alvarez, L. J., Reinach, P. S., and Candia, O. A. (1979) An improved assay for nanomole amounts of inorganic phosphate, *Anal. Biochem. 100*, 95−97.
30. Copeland, R. A. (1996) *Enzymes. A practical introduction to structure, mechanism and data analysis*, VCH Publishers, New York.
31. Menon, A. S., and Goldberg, A. L. (1987) Protein substrates activate the ATP-dependent protease La by promoting nucleotide binding and release of bound ADP, *J. Biol. Chem. 262*, 14929−14934.
32. Menon, A. S., and Goldberg, A. L. (1987) Binding of nucleotides to the ATP-dependent protease La from *Escherichia coli*, *J. Biol. Chem. 262*, 14921−14928.
33. Waxman, L., and Goldberg, A. L. (1986) Selectivity of intracellular proteolysis: protein substrates activate the ATP-dependent protease (La), *Science 232*, 500−503.
34. Waxman, L., and Goldberg, A. L. (1982) Protease La from *Escherichia coli* hydrolyzes ATP and proteins in a linked fashion, *Proc. Natl. Acad. Sci. U.S.A. 79*, 4883−4887.
35. Vasilyeva, O. V., Kolygo, K. B., Leonova, Y. F., Potapenko, N. A., and Ovchinnikova, T. V. (2002) Domain structure and ATP-induced conformational changes in *Escherichia coli* protease Lon revealed by limited proteolysis and autolysis, *FEBS Lett. 526*, 66−70.
36. Smith, C. K., Baker, T. A., and Sauer, R. T. (1999) Lon and Clp family proteases and chaperones share homologous substrate-recognition domains, *Proc. Natl. Acad. Sci. U.S.A. 96*, 6678−6682.
37. Wickner, S., and Maurizi, M. R. (1999) Here's the hook: similar substrate binding sites in the chaperone domains of Clp and Lon, *Proc. Natl. Acad. Sci. U.S.A. 96*, 8318−8320.
38. Bochtler, M., Hartmann, C., Song, H. K., Bourenkov, G. P., Bartunik, H. D., and Huber, R. (2000) The structures of HslU and the ATP-dependent protease HslU−HslV, *Nature 403*, 800−805.
39. Wang, J., Song, J. J., Franklin, M. C., Kamtekar, S., Im, Y. J., Rho, S. H., Seong, I. S., Lee, C. S., Chung, C. H., and Eom, S. H. (2001) Crystal structures of the HslVU peptidase-ATPase complex reveal an ATP-dependent proteolysis mechanism, *Structure 9*, 177−184.
40. Sousa, M. C., Trame, C. B., Tsuruta, H., Wilbanks, S. M., Reddy, V. S., and McKay, D. B. (2000) Crystal and solution structures of an HslUV protease-chaperone complex, *Cell 103*, 633−643.
41. Pate, E., Franks-Skiba, K., White, H., and Cooke, R. (1993) The use of differing nucleotides to investigate cross-bridge kinetics, *J. Biol. Chem. 268*, 10046−10053.
42. Park, S., Ajtai, K., and Burghardt, T. P. (1997) Mechanism for Coupling Free Energy in ATPase to the Myosin Active Site, *Biochemistry 36*, 3368−3372.

BI036165C